2344–2350 Nucleic Acids Research, 1994, Vol. 22, No. 12

Localization of the intrinsically bent DNA region upstream of the *E.coli rrnB* P1 promoter

Tamas Gaal, Lin Rao, Shawn T.Estrem, Jin Yang[1], Roger M.Wartell[1] and Richard L.Gourse*
Department of Bacteriology, University of Wisconsin–Madison, 1550 Linden Drive, Madison, WI 53706 and [1]School of Biology, Georgia Institute of Technology, Atlanta, GA 30332, USA

Received March 3, 1994; Revised and Accepted May 8, 1994

ABSTRACT

DNA sequences upstream of the *rrnB* P1 core promoter (−10, −35 region) increase transcription more than 300-fold *in vivo* and *in vitro*. This stimulation results from a *cis*-acting DNA sequence, the UP element, which interacts directly with the alpha subunit of RNA polymerase, increasing transcription about 30-fold, and from a positively acting transcription factor, FIS, which increases expression another 10-fold. A DNA region exhibiting a high degree of intrinsic curvature has been observed upstream of the *rrnB* P1 core promoter and has thus been often cited as an example of the effect of bending on transcription. However, the precise position of the curvature has not been determined. We address here whether this bend is in fact related to activation of rRNA transcription. Electrophoretic analyses were used to localize the major bend in the *rrnB* P1 upstream region to position approximately −100 with respect to the transcription initiation site. Since most of the effect of upstream sequences on transcription results from DNA between the −35 hexamer and position −88, i.e. downstream of the bend center, these studies indicate that the curvature leading to the unusual electrophoretic behavior of the upstream region does not play a major role in activation of rRNA transcription. Minor deviations from normal electrophoretic behavior were associated with the region just upstream of the −35 hexamer and could conceivably influence interactions between the UP element and the alpha subunit of RNA polymerase.

INTRODUCTION

The P1 promoters of the seven *E.coli* ribosomal RNA operons are among the strongest in the cell with the capacity to produce as much RNA as all the other cellular promoters combined. This exceptional strength results from a near consensus core promoter (−10, −35 region) activated more than 300-fold by an upstream activator region (UAR) (1–3).

The UAR contains two functionally distinct elements (Fig. 1B). A promoter proximal region, the UP element, is a *cis*-acting DNA sequence located between −60 and −40 with respect to the transcription start site which interacts directly with the C-terminal portion of the α subunit of RNA polymerase and increases transcription about 30-fold (2–6 and W.Ross, E.Blatter, R.H.Ebright, and R.L.Gourse, unpublished results). Furthermore, a promoter distal region, located between −150 and −60, increases transcription about 10-fold by binding the FIS protein at three sites (7). FIS Site I, the site closest to the promoter, accounts for 70–80% of the effect of FIS on transcription (7). FIS most likely stimulates transcription by interacting directly with RNA polymerase (6, 8, and A.J.Bokal, W.Ross, and R.L.Gourse, unpublished results).

DNA fragments containing the *rrnB* P1 promoter region have retarded mobility on polyacrylamide gels (1, 9), a feature characteristic of intrinsic DNA curvature (10). DNA curvature is generally believed to be a function of oligo-dA tracts repeated in phase with the DNA helix (11–13), although curvature without A tracts has also been reported (14). It is possible to localize curvature within a fragment by electrophoresis, since DNA fragments in which the bend is at the center are substantially more retarded than fragments with the bend near an end (10, 15, 16). Furthermore, the ratio of the apparent length of a DNA fragment to its actual length can be correlated to an apparent DNA bend angle based on co-electrophoresis of fragments containing A_6 tracts (17, 18). Detection of DNA bending is facilitated by electrophoresis in the cold, by the presence of Mg^{2+} (19), and by high polyacrylamide concentrations (11). The relationship between bending and electrophoretic mobility is most likely an approximation which could also be affected by other structural distortions in DNA (13).

Predictions from computer analyses indicate that bent DNA sequences often occur in the 5′ flanking regions of protein coding sequences (20) and are preferentially located upstream of strong *E.coli* promoters (21). Direct cloning of fragments displaying unusual electrophoretic mobility also suggested that curvature is often associated with promoters (22). A+T-rich upstream DNA displaying curvature can sometimes replace a transcriptional activator (e.g. see 23–25). However, in some cases it has not been shown that the position of the bend and the position of the sequences which increase transcription are the same. Furthermore, when the sequences do overlap, it is difficult to distinguish effects of curvature on RNAP activity (e.g. by

*To whom correspondence should be addressed

facilitating RNAP binding or DNA strand opening) from effects of the A+T-rich sequences on transcription independent of the curvature.

In this report, we address the relationship between rRNA transcription activity and DNA bending by identification of the sequences required for DNA curvature and comparison of those regions with information now available about the regions required for stimulation of transcription of *rrnB* P1 (2, 3, 7). Our results suggest that the large intrinsic curvature in the vicinity of the *rrnB* P1 promoter does not play a major role in rRNA transcription.

MATERIALS AND METHODS

General methods

Plasmid DNA was purified using Qiagen columns (Qiagen Inc.), phenol extracted, and ethanol precipitated. Restriction enzymes and linkers were obtained primarily from New England Biolabs, and sequencing primers were provided by the NutraSweet Co. (Mt Prospect, Illinois). All plasmid constructions were confirmed by DNA sequencing using Sequenase (USB).

Plasmids

Restriction fragments are referred to by their *rrnB* P1 DNA endpoints (with respect to the transcription start site, +1). Eight bp *EcoRI* and 12 bp *BamHI* linkers were ligated to the upstream and downstream ends, respectively, of a fragment containing the *rrnB* P1 sequences from −154 (*AluI*) to −28 (*HaeIII*), and inserted into the *EcoRI* and *BamHI* sites of pUC19 and pRW4 to make pJNBend130 and pJY237, respectively (J.T.Newlands, R.L.Gourse, J.Yang, and R.M.Wartell, unpublished results). Fragments indicated in Table I were generated by digestion of these plasmids with *EcoRI* (−154), *BamHI* (−28), *DraI* (−46), and *TaqI* (−104 and −114). Other restriction fragments (illustrated in Figure 1B) were obtained as *EcoRI*−*HindIII* fragments from previously existing plasmids (3, and L.Rao and R.L.Gourse, unpublished results), and inserted between the unique *EcoRI* and *HindIII* sites of the permutation vector pSL6 (8), a derivative of pBEND2 (16) (Figure 1A).

Analysis of DNA bending by polyacrylamide gel electrophoresis

Fragments from pJY237 were examined at 25°C on 8% acrylamide:bisacrylamide (29:1) gels in 1×TBE buffer (26) for 8.5 hours at 5−7 V/cm as described (17). *HaeIII* and *HinfI* digested pBR322 served as size standards. pSL6 derivatives were digested separately with at least seven different restriction enzymes to generate a set of fragments of equal length containing the promoter DNA segment of interest at different positions within the restriction fragment. The fragments were electrophoresed on 220×200×1.5 mm 10% acrylamide: bisacrylamide (30:1) gels in 0.5×TBE buffer at 3V/cm for 48 hours at 6°C. A *HaeIII* digest of pUC19 was used as a molecular weight standard. As controls, identical digests were run under conditions where bent and non-bent fragments migrate similarly, e.g. in the presence of 0.5 μg/ml ethidium bromide or at 55°C (25 V/cm) (27). After electrophoresis, gels were stained with ethidium bromide and photographed with UV illumination. The apparent length of each fragment was determined from semi-logarithmic plots of molecular weight versus migration distance and expressed as a ratio of the fragment's actual size (K value).

The errors in determining a K value for a specific fragment between different experiments were usually quite small (≤ 4%). Furthermore, differences in electrophoretic mobility between fragments of the same size but with either different sequence composition or different endpoints could be detected and visualized reproducibly when the fragments were in adjacent gel lanes or within the same gel lane. Thus, differences in the mobilities of fragments in certain DNA regions which have K values very close to 1.0 (zero curvature) could still be detected reproducibly.

Construction of mutations in the UP element and evaluation of their effects on promoter strength

Mutations were constructed using the method of Kunkel (28). Primer 5′-ATTTAAAATAATATTCTGACCGCG-3′ was used to create a substitution of a T for an A at position −55 (A−55T). Primer 5′-GACAAGAGGAATATTAAAATAATT-3′ was used to create the double substitution T−43A, A−44T. Operon fusions with *lacZ* were constructed in strain NK5031, and β-galactosidase activities were measured as described previously (29).

RESULTS

Detection of bending by electrophoresis

Intrinsic DNA curvature can be identified by unusual electrophoretic behavior. The K value is the ratio of the apparent length of a fragment to its actual length: the greater the K value, the larger the deviation in apparent size from real size, which can be indicative of an increase in the bend angle. The K value is also a function of acrylamide concentration, electrophoresis conditions, the length of the DNA fragment, and the position of the bend within the fragment (10, 15−19). The closer the bend is to the center of the fragment, the slower is the electrophoretic mobility.

An rRNA promoter containing *rrnB* P1 endpoints −154 to +50 with respect to the transcription initiation site was shown previously to have maximum rRNA transcription activity and to migrate aberrantly on acrylamide gels (1). K values of the *rrnB* P1 sub-fragments listed in Table 1 were determined at 25°C and indicated that an anomalous structure, perhaps a bend, was located between −154 and −46. Assuming the anomalous structure represents DNA bending, these data were not sufficient to determine the distribution of the curvature within this region nor the location of the bend center. However, the −154 to −114 and −104 to −46 sub-fragments had normal mobilities, suggesting that the endpoints in the −100 region either disrupted the curved region or placed it too close to the end of the fragment

Table 1. K Values for restriction fragments containing UAR DNA

fragment endpoints[a]	K value[b]
−154 to −28	1.29
−154 to −46	1.20
−104 to −28	1.05
−104 to −46	1.00
−154 to −114	1.00

[a]*rrnB* P1 sequence coordinates. +1 is the transcription initiation site.
[b]The K value is the apparent electrophoretic mobility relative to the actual size of the fragment. Electrophoresis was performed at 25°C.

to affect electrophoretic migration substantially. The K value of 1.29 for the −154 to −28 fragment resulted in an estimate of a bend angle of approximately 108° when calculated using the empirical equations developed by Koo and Crothers (17) for DNAs with A_6 tracts, a value of 18° per A_6 tract (30, 31), and a value of 10.5 bp/helix turn (i.e. the retarded mobility of this region was equivalent to that which would be afforded by six A_6 tracts).

We next analyzed the rRNA promoter region using the permutation vector pSL6 (8, 16) illustrated in Figure 1A. Fragments of DNA associated with different functionally important sequences in the region of the *rrnB* P1 promoter (Figure 1B) were cloned between the two tandem repeats in the vector. Cleavage at different restriction sites in the tandem repeat generated fragments of the same absolute length but with the bend (if present) at different positions with respect to the ends. The apparent sizes of the fragments were then determined by electrophoresis. Since multiple bends within a fragment can limit the usefulness of this technique, we examined relatively short pieces of DNA.

A set of at least seven different restriction digestions was performed on plasmid constructs containing each *rrnB* insert. The set of digests containing a single *rrnB* insert was electrophoresed on a 10% polyacrylamide gel at 6°C alongside known length markers (data not shown). The digests generating the slowest and fastest running fragments from each permuted fragment set were then electrophoresed on the same gel to permit direct comparison of the K values of different *rrnB* inserts. The results are shown in Figure 2A, illustrated graphically in Figure 3A, and tabulated in Table 2. Only the fragment containing the −154 to −64 insert (and the larger fragments which contain this region, −154 to −46 and −154 to +50) had K values of 1.4 to 1.5. All other fragments tested, including several containing the UP element region with a variety of fragment endpoints, deviated in mobility from their actual sizes by less than or equal to about 10%. These results indicated that the major bend in the *rrnB* P1 promoter region is located upstream of the UP element.

Electrophoresis of the same digests in the presence of 0.5 μg/ml ethidium bromide or at 55°C, either of which reduces the effect of bending on electrophoretic mobility (32), results in migration

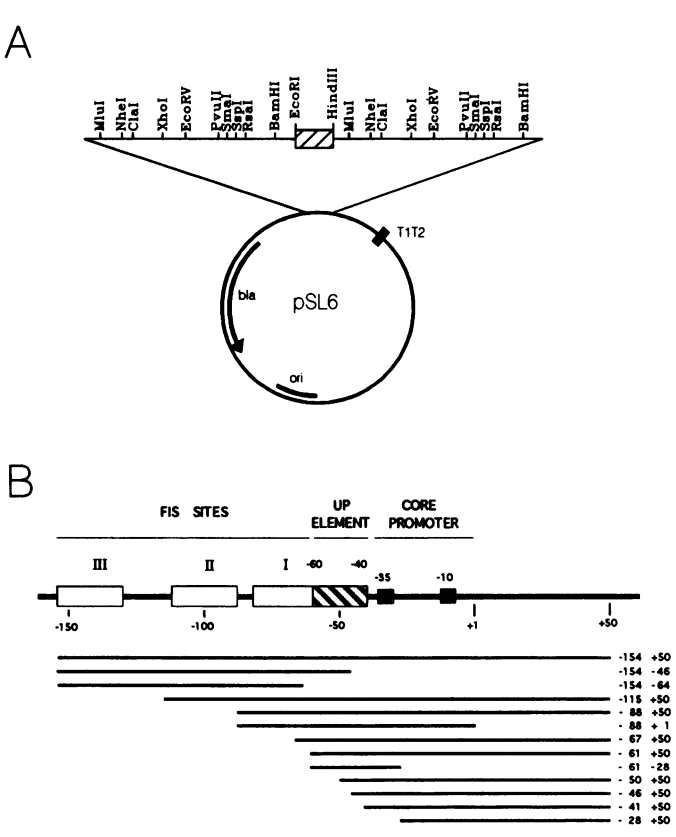

Figure 1. **(A)** Plasmid pSL6 (8). The plasmid has two identical regions of DNA containing multiple restriction sites flanking *EcoRI* and *HindIII* sites for promoter fragment insertion (hatched box). T1T2: transcription termination region from *rrnB*. bla: ampicillin resistance gene. ori: origin of DNA replication. **(B)** The *rrnB* P1 promoter region and DNA fragments used for permutation analysis. The core promoter region, UP element, and FIS binding sites are indicated (2, 3, 7). The endpoints of *rrnB* fragments inserted into pSL6 are shown on the right. The resulting plasmids are listed in Table 2. The fragments are displayed under the schematic in order to illustrate the functionally relevant regions contained within each fragment.

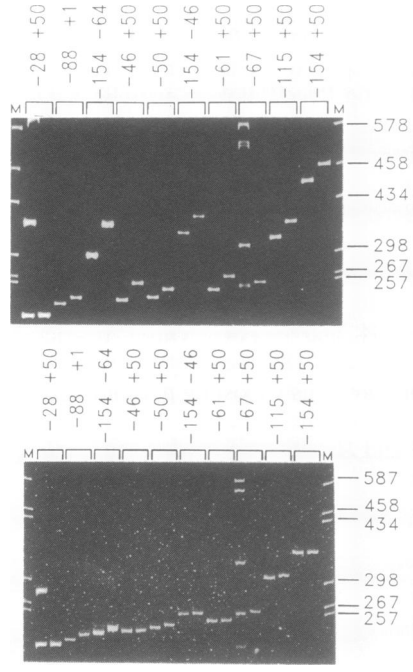

Figure 2. Gel electrophoresis of permuted fragments of *rrnB* P1. **(A)** electrophoresis performed at 6°C. **(B)** electrophoresis performed at room temperature in the presence of 0.5 μg/ml ethidium bromide. In each digest, the *rrnB* insertion is embedded within 137 bp of vector DNA. The two restriction digests resulting in the maximal and minimal electrophoretic mobilities of each permuted fragment set were run on the same gel. Plasmid DNAs used in each lane are identified by the endpoints of their *rrnB* DNA. The top of the gel is not pictured. Restriction enzymes used in each lane were: M: pUC19 digested with *HaeIII* (molecular weight standard; sizes of the fragments in base pairs are indicated at the right of each panel); −28 to +50: *SspI*, *MluI*. (*SspI* cleaves at multiple sites within the vector resulting in additional higher molecular weight bands); −88 to +1: *MluI*, *PvuII*; −154 to −64: *MluI*, *SmaI*; −46 to +50: *BamHI*, *XhoI*; −50 to +50: *BamHI*, *XhoI*; −154 to −46: *BamHI*, *EcoRV*; −61 to +50: *BamHI*, *MluI*; −67 to +50: *RsaI*, *MluI*. (*RsaI* cleaves at multiple siteswithin the vector resulting in additional bands. The *rrnB* sequences are contained within the fragment migrating near the position of the 257 and 267 bp standards.); −115 to +50: *BamHI*, *EcoRV*; −154 to +50: *BamHI*, *MluI*.

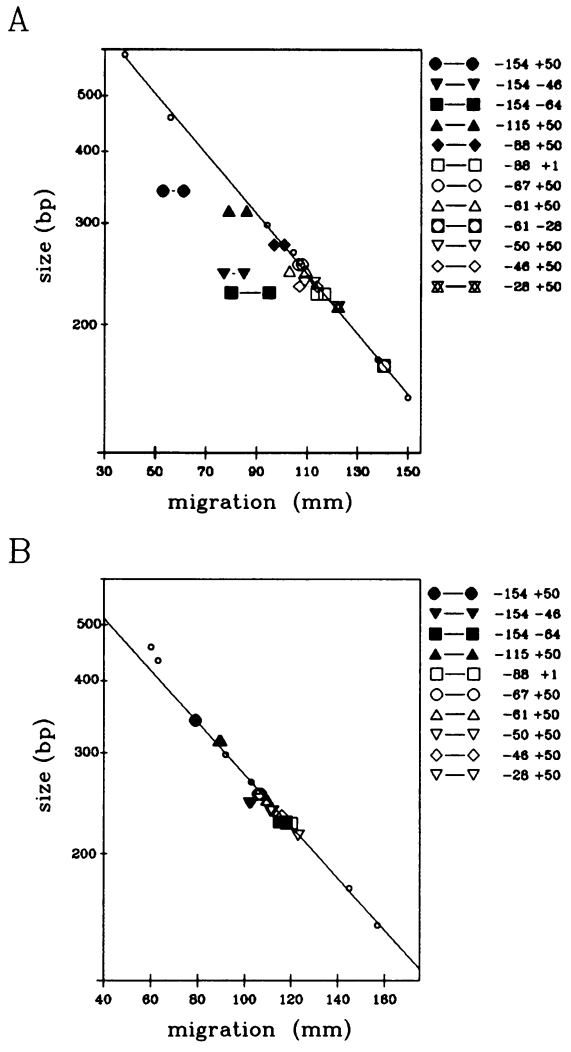

Figure 3. Graphical representation of data pictured in Figure 2. **(A)** Data from electrophoresis performed at 6°C. **(B)** Data from electrophoresis performed at room temperature in the presence of 0.5 μg/ml ethidium bromide. Apparent fragment length in bp is plotted versus distance migrated in mm. A line is drawn through points (small dots) derived from the molecular weight standard. The pair of symbols corresponding to the maximum and minimum apparent lengths of fragments from each permuted set are connected. The symbols for each set are defined on the right side of the graph. From this graphical representation, it is apparent that the fragments containing *rrnB* sequences −154 to +50, −154 to −46, and −154 to −64 migrate substantially slower at 6°C than expected from their lengths.

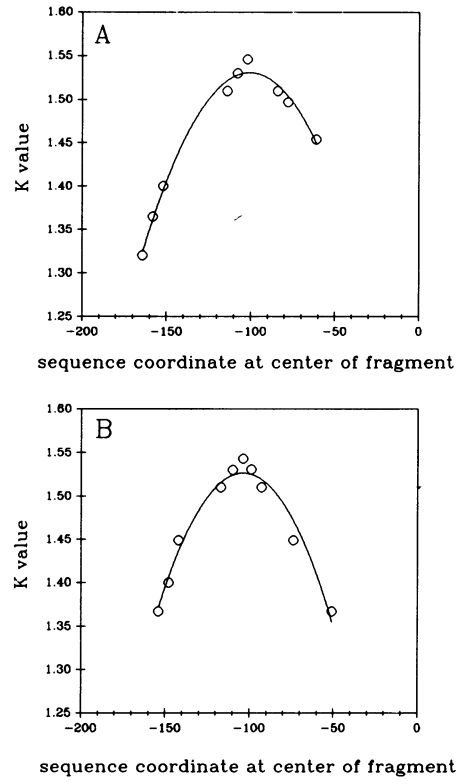

Figure 4. Identification of the major bend center. **(A)** Digests of plasmid pLR18 (−154 to −64 fragment) and **(B)** pLR20 (−154 to −46 fragment). Digests were electrophoresed at low temperature as described above. Each point on the graph represents the K value of one member of the permuted set (containing either the −154 to −64 or the −154 to −46 insert) as a function of the coordinate at the fragment's center. The restriction enzymes used were (A) *MluI, BglII, NheI, EcoRV, PvuII, SmaI, SspI, RsaI, BamHI*; and (B) *MluI, BglII, NheI, XhoI, DraI, EcoRV, PvuII, SmaI, SspI, BamHI*. The apex of the curve indicates the position of the bend center (16). Sample calculation: the −154 to −64 fragment was inserted between the tandem repeats in the bend vector. When the plasmid was cut with *PvuII* (one of the enzymes generating a fragment with a high K value), the resulting 227 bp fragment had approximately 66 bp on the left of the 90 bp insert containing the promoter and 71 bp on the right of the insert. The center of the fragment is about 113 bp from each end, or at about position −107 with respect to the transcription start site.

almost as predicted by the actual fragment sizes (Figure 2B, Figure 3B, Table 2, and data not shown). Thus, deviations from normal mobility are a function of the structure of the fragment and not from miscalculation of actual length.

The electrophoretic mobility of the −154 to −64 fragment was also compared directly with that of fragments containing different numbers of phased A tracts from the Thompson−Landy set (18) in order to obtain an estimate of the major bend angle occurring within the *rrnB* promoter region. The −154 to −64 fragment migrated with a K value between that of fragments with 4 and 5 A-tracts, providing an estimated bend angle of about 80° (18). This estimate of 80° and that noted above of 108° likely define a range for the real bend angle, considering the limitations of the two methods.

Position of the major bend

The mobility of a DNA fragment depends on the position of the bend relative to the center of the fragment. To identify where within the −64 to −154 region the bend resides, the data obtained from a set of 9 different digests of the vector containing the −154 to −64 fragment and a set of 10 different digests of that containing the −154 to −46 fragment were plotted as Figures 4A and 4B, respectively. In these figures, the K value for each of the fragments in the set was plotted against the sequence coordinate at the center of the fragment. The fragments with the highest K value are those where the center of the fragment is at approximately −100, thereby identifying this position as the bend center. This position is well upstream of both the UP element and FIS Site I, the major upstream determinants of promoter strengh at *rrnB* P1.

Table 2. K values from circular permutation experiments[a]

plasmid	rrnB P1 endpoints	actual size (bp)[b]	apparent size (bp)[c]		K values[d]	
			6°C	Etbr	6°C	Etbr
pSL6	−154+50	(341)	440 − 484	356 − 356	1.29 − 1.42	1.04 − 1.04
pLR20	−154−46	(245)	328 − 365	264 − 270	1.34 − 1.49	1.08 − 1.10
pLR18	−154−64	(227)	293 − 350	227 − 232	1.29 − 1.54	1.00 − 1.02
pSL8	−115+50	(302)	328 − 353	309 − 315	1.09 − 1.17	1.02 − 1.04
pSL9	−88+50	(275)	267 − 289	nd[e]	0.97 − 1.05	nd
pSL13	−88+1	(226)	224 − 233	221 − 226	0.99 − 1.03	0.98 − 1.00
pSL10	−67+50	(254)	249 − 254	249 − 254	0.98 − 1.00	0.98 − 1.00
pSL11	−61+50	(248)	246 − 265	245 − 248	0.99 − 1.07	0.99 − 1.00
pLR1	−61−28	(170)	170 − 177		nd	1.00 − 1.04
pSL12	−50+50	(237)	235 − 246	237 − 240	0.99 − 1.04	1.00 − 1.01
pLR21	−46+50	(233)	233 − 256	230 − 230	1.00 − 1.10	0.99 − 0.99
pLR9	−41+50	(228)	217 − 233		nd	0.95 − 1.02
pLR19	−28+50	(215)	219 − 219	210 − 215	1.02 − 1.02	0.98 − 1.00

[a]As described in Materials and Methods and in text.
[b]In each case, the *rrnB* insertion is embedded within 137 bp of vector DNA.
[c]Minimum and maximum apparent lengths of a set of permuted fragments of the same size with different endpoints, from electrophoresis at 6°C or in the presence of ethidium bromide (Etbr).
[d]Minimum and maximum K values (apparent size/actual size) of a set of permuted fragments of the same size with different endpoints, from electrophoresis at 6°C or in the presence of ethidium bromide (Etbr). The K values represent the range of mobilities for a given fragment set. Errors in K value determination are within 4% (see Methods).
[e]nd: not determined.

Minor deviations from linearity in fragments not containing the major bend

Examination of fragments downstream of the major bend locus (−67 to +50; −61 to +50; −50 to +50; −46 to +50) did not lead to a simple interpretation of curvature in this region. For example, the −67 to +50 fragment migrates more normally than the −61 to +50 or −46 to +50 fragments. It is possible that there are multiple small deviations from linearity caused by these sequences (or by the sequences created at the *rrnB*-vector junctions), some of which compensate for one another by bending in opposite directions.

We tested whether these minor electrophoretic abnormalities reflect curvature in the UP element (−40 to −60) region by comparing the mobility of a fragment with −88 to +1 *rrnB* endpoints to that of an identical fragment containing a substitution of the sequences from −41 to −59 [the SUB mutation, sequence provided in legend of Figure 5 (2, 3)]. The wild type fragment ('W'; Figure 5), which contains two A-tracts in phase, migrated only slightly slower than the fragment of the same length containing the SUB mutation ('S'), consistent with the results reported in Table 2 indicating that only minor curvature exists in this region. (The maximum K value of the wild type fragment was about 1.03, while the K value of the SUB fragment was about 0.98.) The small difference in the mobilities of the wild type and SUB fragments is likely to reflect bending, however, since the difference was greatest when the A-tract regions were near the center of the fragment (Figure 5, *PvuII* or *XhoI* digests).

Functional role of A-tracts within the UP element

The UP element consists of 90% adenine and thymine residues, contains phased A/T-tracts (Figure 6), and increases transcription of *rrnB* P1 at least 30-fold *in vivo* and *in vitro* (2, 3). Replacement of the −40 to −60 region in *rrnB* P1 with the SUB mutation completely eliminates activation by the UP element and partially reduces activation by FIS bound at FIS Site I (3), resulting in a reduction of transcription even greater than 30-fold.

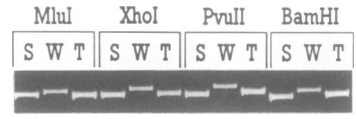

Figure 5. Electrophoretic mobility of fragments containing *rrnB* P1 derivatives with substitutions upstream of the −35 hexamer. Promoter fragments with *rrnB* P1 sequences from −88 to +1 were inserted into pSL6 and digested with either *MluI*, *XhoI*, *PvuII*, or *BamHI*. S, SUB mutant (2, 3); W, wild type; T, C−37T substitution (29, 34). Electrophoresis was performed at 6°C as described for the other figures. The sequence of the SUB mutation in the UP element of *rrnB* P1 is (−59) 5′-GACTGCAGTGGTACCTAGG-3′ (−41) (3).

The functional role of the phased A/T-tracts in the −40 to −60 region was addressed by disrupting the A/T-tracts with substitution mutations without changing the A+T content. The T-tract at −41 to −43 and the A-tract at −44 to −46 (top strand sequences provided in Figure 6) were altered with a double substitution (T−43A, A−44T). In a separate experiment, the −54 to −57 A-tract was disrupted with a single substitution, A−55T. The mutant promoters (with *rrnB* endpoints of −88 to +1) were fused to *lacZ* and inserted into the bacterial chromosome as monolysogens of bacteriophage lambda. The activities of these fusions are shown in Table 3, compared to a fusion with the wild type promoter with the same endpoints. The A/T-tract mutations reduce transcription only 1.3 to 1.6 fold, implying that the continuous runs of A or T residues do not account for the 30-fold effect of the UP element.

Altered DNA structure from a mutation at −37

We have reported previously that a mutation at position −37 (C−37T) reduces *rrnB* P1 promoter activity 10−20 fold, but that substitution of an A or G residue at this position reduces activity only 2−3 fold (29, 34). We speculated that the large allele-specific effect of the T substitution might result not from

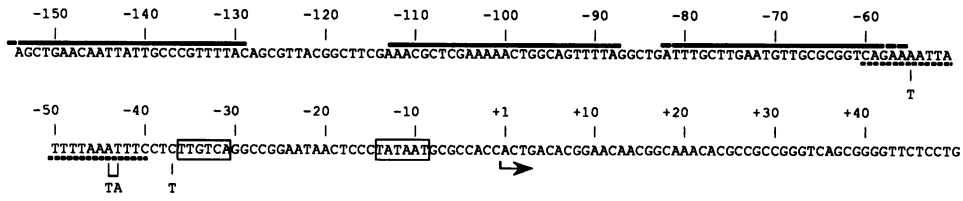

Figure 6. DNA sequence of the *rrnB* P1 region [from (33)]. The three FIS Sites are indicated above the sequence, the UP element is indicated below the sequence as a broken line, the −10 and −35 hexamers are boxed, and the transcription start site is indicated by an arrow. The substitutions described in the text at positions −37, −43, −44, and −55 are also indicated.

the importance of the wild type C residue to promoter function, but from the creation of a series of four T residues in phase with another T tract upstream, which might result in a bend that might be detrimental to promoter function *in vivo*.

In order to test this hypothesis, we compared the mobility of the promoter fragment containing the wild type −88 to +1 region with that of the same promoter fragment containing the C−37T mutation at position −37. As shown in Figure 5, the fragment containing the C−37T mutation ('T') migrates differently from that containing the wild type promoter region. Whether or not this alteration in structure actually is responsible for the defect in promoter activity of course remains to be determined. Since the C−37T promoter fragment migrates more like that containing the SUB mutation, the newly created A/T tract may be out of phase with other A/T tracts in the fragment. The resulting bends in opposing directions might then cancel overall effects on mobility.

DISCUSSION

Using permuted sets of restriction fragments carrying different portions of the *rrnB* P1 promoter and its upstream sequences we were able to localize a major structural anomaly, most likely a bend, centered around position −100. This conclusion agreed with the results of other electrophoretic analyses of the *rrnB* promoter region [Table 1 and (1)], and with conclusions based on the electrophoretic behavior of fragments containing linker scanning mutations in the upstream sequence (9). However, this bend is unlikely to play a prominent role in *rrnB* P1 transcription, since it is upstream of the sequences responsible for UP element function, growth rate dependent regulation, or stringent control of this promoter (1, 3, 35, 36 and C.A.Josaitis and R.L.Gourse, unpublished results). Likewise, the bend is upstream of FIS Site I, which accounts for the majority of FIS-mediated activation (7). It is conceivable, however, that the bend at about −100 could have a role in mediating the small effects on transcription activation attributable to FIS Sites II and III.

Two methods used to estimate the intrinsic bend angle resulted in a range of values from 80−108°. Both methods rely on certain problematical assumptions [see (17, 37)], but the presence of the upstream region gives DNA fragments a K value equivalent to that expected from the presence of four to six phased A_6 tracts. Figure 6 shows that there are five A (or T)-tracts 3bp or more in length (at −81, −92, −104, −113, and −134) in the vicinity of the bend center. Other sequences could add to the degree of curvature observed, and/or anomalies in structure in addition to bending could also contribute to the observed retarded electrophoretic mobility. Nevertheless, the position of the bend does not correlate with the region responsible for transcription activation, and as a result, we have not attempted to extend the structural analysis further in order to resolve these questions. The estimate of the bend angle, but not the bend position, should thus be regarded as tentative.

Table 3. Expression of fusions with A tract mutations

Promoter[a]	β-gal activity[b]
wild type	4970 ± 140
T−43A A−44T	3850 ± 177
A−55T	3030 ± 192

[a]Promoter−*lacZ* fusions are described in the text.
[b]Miller units. Under comparable conditions, the SUB mutation eliminating UP element function reduces β-galactosidase activity more than 30-fold (3).

The region upstream of −60 in each of the seven *rrn* operons contains multiple phased A/T tracts which might be expected to lead to unusual electrophoretic mobility (21) [see (38) for sequences]. However, the phased A/T tracts are not in exactly the same position as those that generate the bend centered at about −100 in *rrnB*, nor are they uniformly positioned relative to the core promoter. Therefore, their function, if any, remains unknown.

Fragments containing at least a portion of the *rrnB* UP element but without the −100 region exhibited a slight degree of aberrant electrophoretic mobility (R values less than or equal to 1.1, which is less than or equal to the deviation expected from the presence of two phased A/T tracts under our conditions). A mutation at position −37 which creates a T-tract increased the electrophoretic mobility of an *rrnB* P1 promoter fragment slightly, further indicating that a subtle, non-standard DNA structure probably exists in this region.

Three point mutations disrupting the A/T tracts in the wild type UP element had only small effects on transcription activity. Therefore, if the A/T tracts are responsible for the small degree of curvature associated with this region, either the mutations do not affect this curvature, or the curvature plays little role in the 30-fold increase in transcription resulting from UP element function. On the other hand, either displacement of the UP element by non-integral portions of a helical turn (6, 29, 34) or creation of an additional T tract with a T substitution at position −37 (29, 34) severely decreases promoter activity. Thus, correct positioning of the RNAP alpha subunit (which binds to the UP element) relative to the sigma subunit (which binds to the −10 and −35 hexamers) most likely plays a major role in promoter activity (2). The sequence and structural determinants responsible

for interaction of the RNA polymerase alpha subunit with the −40 to −60 region and thus for UP element function are under investigation. Although a high degree of intrinsic curvature appears not to play a role in this interaction, it is certainly possible that binding of alpha may be facilitated by subtle structural distortions determined by the DNA sequence.

In summary, although the obvious intrinsic curvature in the *rrnB* P1 upstream region is often cited as an example of the effects of DNA bending on transcription, apparently this bend plays little or no role in FIS-dependent activation, UP element function, or in core promoter strength, which together account for the high activity of rRNA promoters.

ACKNOWLEDGEMENTS

We thank Janet Newlands and the late Sigrid Leirmo for contributions in the initial stages of these studies, David Wheeler for discussions on computer modeling, and Wilma Ross for critical reading of the manuscript. This work was supported by research grants GM37048 (R.L.G.) and GM38045 (R.M.W.) from the National Institutes of Health and by an NIH predoctoral training grant (S.T.E.).

REFERENCES

1. Gourse, R.L., deBoer, H.A. and Nomura, M. (1986) *Cell* **44**, 197−205.
2. Ross, W., Gosink, K.K., Salomon, J., Igarashi, K., Zou, C., Ishihama, A., Severinov, K. and Gourse, R.L. (1993) *Science* **262**, 1407−1413.
3. Rao, L. Ross, W., Appleman, J.A., Gaal, T., Leirmo, S., Schlax, P.J., Record, M.T. Jr. and Gourse, R.L. (1994) *J. Mol. Biol.* **235**, 1421−1435.
4. Leirmo, S. and Gourse, R.L. (1991) *J. Mol. Biol.* **220**, 555−568.
5. Newlands, J.T., Ross, W., Gosink, K.K. and Gourse, R.L. (1991) *J. Mol. Biol.* **220**, 569−583.
6. Newlands, J.T., Josaitis, C.A., Ross, W. and Gourse, R.L. (1992) *Nucleic Acids Res.* **20**, 719−726.
7. Ross, W., Thompson, J.F., Newlands, J.T. and Gourse, R.L. (1990) *EMBO J.* **9**, 3733−3742.
8. Gosink, K.K., Ross, W., Leirmo, S., Osuna, R., Finkel, S.E., Johnson, R.C. and Gourse, R.L. (1993) *J. Bacteriol.* **175**, 1580−1589.
9. Zacharias, M., Goringer, H.U. and Wagner, R. (1992) *Biochem.* **31**, 2621−2628.
10. Wu, H.-M. and Crothers, D.M. (1984) *Nature* **308**, 509−513.
11. Marini, J.C., Levene, S.D, Crothers, D.M and Englund, P.T. (1982) *Proc. Natl. Acad. Sci. USA* **79**, 7664−7668.
12. Trifonov, E.N. (1985) *CRC Crit. Rev. Biochem.* **19**(2), 89−106.
13. Hagerman, P.J. (1990) *Annu. Rev. Biochem.* **59**, 755−781.
14. Bolshoy, A., McNamara, P., Harrington, R.E. and Trifonov, E.N. (1991) *Proc. Natl. Acad. Sci. USA* **88**, 2312−2316.
15. Prentki, P., Pham, M.H. and Galas, D.J. (1987) *Nucleic Acids Res.* **15**, 10060.
16. Kim, J., Zwieb, C., Wu, C. and Adhya, S. (1989) *Gene* **85**, 15−23.
17. Koo, H.-S. and Crothers, D.M. (1988) *Proc. Natl. Acad. Sci. USA* **85**, 1763−1767.
18. Thompson, J.F. and Landy, A. (1988) *Nucleic Acids Res.* **16**, 9687- 9705.
19. Diekmann, S. and James,C.W. (1985) *J.Mol.Biol.* **186**, 1−11.
20. VanWye, J.D., Bronson, E.C. and Anderson, J.N. (1991) *Nucleic Acids Res.* **19**, 5253−5261.
21. Plaskon, R.R. and Wartell, R.M. (1987) *Nucleic Acids Res.* **15**, 785−796.
22. Tanaka, K., Muramatsu, S., Yamada, H. and Mizuno, T. (1991) *Mol. Gen. Genet.* **226**, 367−376.
23. Gartenberg, M.R. and Crothers, D.M. (1991) *J. Mol. Biol.* **219**, 217−230.
24. Bracco, L., Kotlarz, D., Kolb, A., Diekmann, S. and Buc, H. (1989) *EMBOJ.* **8**, 4289−4296.
25. Nachaliel, N., Melnick, J., Gafny, R. and Glaser, G. (1989) *Nucleic Acids Res.* **17**, 9811−9822.
26. Peacock, A.C. and Dingman, C.W. (1968) *Biochem.* **7**, 668−674.
27. Diekmann, S. (1992) *Meth. Enzymol.* **212**, 30−46.
28. Kunkel, T. A. (1985). *Proc. Natl. Acad. Sci. USA* **82**, 488−492.
29. Gaal, T., Barkei, J., Dickson, R.R., deBoer, H.A., deHaseth, P.L., Alavi, H. and Gourse, R.L. (1989) *J. Bacteriol.* **171**, 4852−4861.
30. Levene, S.D., Wu, H.-M., and Crothers, D.M. (1986) *Biochem.* **25**, 3988−3995.
31. Griffith, J., Bleyman, M., Rauch, C.A., Kitchin, P.A., and Englund, P.T. (1986) *Cell* **46**, 717−724.
32. Diekmann, S. and Lilley, D.M. (1987) *Nucleic Acids Res.* **15**, 5765−5774.
33. Brosius, J., Dull, T.J., Sleeter, D.D., and Noller, H.F. (1981) *J. Mol. Biol.* **148**, 107−127.
34. Josaitis, C.A., Gaal, T., Ross, W. and Gourse, R.L. (1990) *Biochim. Biophys. Acta* **1050**, 307−311.
35. Dickson, R.R., Gaal, T., deBoer, H.A., deHaseth, P.L. and Gourse, R.L. (1989) *J. Bacteriol.* **171**, 4862−4870.
36. Zacharias, M., Goringer, H.U. and Wagner, R. (1989) *EMBO J.* **8**, 3357−3363.
37. Haran, T.E. and Crothers, D.M. (1989) *Biochem.* 28, 2763−2767.
38. Condon, C., Philips, J., Fu, Z.Y., Squires, C. and Squires, C.L. (1992) *EMBO J.* **11**, 4175−4185.